Available online at www.sciencedirect.com
ScienceDirect
Physica E 40 (2008) 467–473
PHYSICA E
www.elsevier.com/locate/physe

Synthesis and characterization of spray pyrolysed $MgIn_2O_4$ spinel thin films for novel applications

A. Moses Ezhil Raj[a], B. Subramanian[b], V. Senthilkumar[c], M. Jayachandran[b], C. Sanjeeviraja[c,*]

[a]*Departments of Physics, Scott Christian College, Nagercoil 629 003, India*
[b]*ECMS Division, Central Electrochemical Research Institute, Karaikudi 630 006, India*
[c]*Department of Physics, Alagappa University, Karaikudi 630 003, India*

Received 12 January 2007; received in revised form 1 July 2007; accepted 3 July 2007
Available online 25 August 2007

Abstract

A novel ternary oxide compound magnesium indate film, $MgIn_2O_4$ (MIO), manifesting high transparency and conductivity has been prepared by spray pyrolysis technique. Stoichiometrically mixed precursors were thermally sprayed onto glass substrates and decomposed at 400 and 450 °C and the growth parameters were studied in detail. X-ray diffraction (XRD) and Fourier transform infrared (FT-IR) studies have been conducted to confirm the formation of stoichiometric films. The dc electrical conductivity of these films was measured in the temperature range between 30 and 100 °C by four-probe technique. Measurement of Hall coefficient showed n-type electrical conduction and high-carrier concentration. Optical properties were studied in the wavelength range 280–1500 nm and surface morphology of the MIO films were analyzed by scanning electron microscopy (SEM) and, atomic force microscopy (AFM).

PACS: 73.61.Jc; 61.10.Nz; 07.07.Df; 78.66.−w; 68.37.Hk; 68.37.Ps

Keywords: Thin films; XRD; Electrical; Optical; SEM; AFM

1. Introduction

In recent years, considerable attention has been given to wide-gap semiconductors, particularly in the development of transparent and electroconductive oxides. Despite their large bandgaps (>3 eV), they can sustain a high concentration of electrons with a high carrier mobility. The most commonly used post-transition-metal oxides (ZnO, SnO_2 and In_2O_3) are thus serving as transparent conducting oxide (TCO) electrodes in optoelectronic devices [1,2]. However, the recent growing demands for high-performance and low-cost TCO has led to an extensive search for new and novel TCO materials with higher transparency and conductivity [3–5].

A hypothesis has been proposed for finding new transparent and electroconductive oxides [6]. According to these hypothesis, new TCOs like; magnesium indium oxide, $MgIn_2O_4$ (MIO) [7], $CdGa_2O_4$ [8], $ZnGa_2O_4$ [9], Zn_2SnO_4 [10] and few more have been studied recently. Among these ternary oxides, $MgIn_2O_4$ thin films find potential application as a new transparent as well as active electrode in photo-electrochemical solar cells [11]. It is an n-type wide-bandgap semiconductor, which has a separate conducting path in the crystal lattice. It has the general structure like the mineral spinel $MgAl_2O_4$ with the formula AB_2O_4. It falls under inverse spinel category according to the lattice substitution of A and B cations in the tetrahedral and octahedral voids in the fcc–cp oxygen sub-lattice. Unit cell of $MgIn_2O_4$ contains eight formula units ($Z = 8$) corresponding to formula $Mg_8In_{16}O_{32}$. The co-ordination environments of Mg^{2+} and In^{3+} are entirely different from normal spinel because they are introduced into the inverse spinel structure.

*Corresponding author. Tel.: +91 4565 230251; fax: +91 4565 225202.
E-mail address: sanjeeviraja@rediffmail.com (C. Sanjeeviraja).

1386-9477/$ - see front matter © 2007 Elsevier B.V. All rights reserved.
doi:10.1016/j.physe.2007.07.004

An interesting phenomena observed in this spinel structure is that the number of cations occupying the 8a and 16d sites may vary. Half of the In^{3+} ions are placed in tetrahedral 8a sites. The other half of In^{3+} ions and all the Mg^{2+} ions are occupying the octahedral 16d sites due to which the occupancy of them observed is distorted. Intermediate phases also exist with the formula $(A_{1-x}B_x)[A_xB_{2-x}]O_4$ [12]. These films are found to exhibit higher values of electrical conductivity due to electrons generated from oxygen vacancies even without intentional doping [13] and/or from implanting Li^+ and H^+ ions into the crystal lattice [6].

Preparation of such thin films on glass substrate is essentially important for estimating their reproducible and reliable structural, optical and electrical properties. Different techniques of deposition have been reported for preparing $MgIn_2O_4$ by pulsed laser deposition [14], combustion synthesis [15] and magnetron sputtering [16–18]. Spray pyrolysis is a simple and elegant technique for large area preparation of TCO thin films and as far as we know, spray pyrolysis preparation of $MgIn_2O_4$ has not yet been reported. In the present paper, the preparation of MIO spinel thin films by spray pyrolysis technique and their structural, electrical, surface morphology and optical properties are reported.

2. Experimental details

The spray pyrolysis setup and the detailed procedure adopted for the deposition of MIO thin films have been described elsewhere [19]. $MgIn_2O_4$ thin films were prepared by spraying an alcoholic solution containing magnesium acetate $Mg(CH_3COO)_2 \cdot 4H_2O$ and indium chloride $InCl_3 \cdot 3H_2O$ in stoichiometric (1:2) proportion on to heated glass substrates. The spray solution was always buffered by a small amount of hydrochloric acid to increase the solubility of the solution. The required deposition parameters to obtain high-quality films were optimized by controlling the associated process parameters and are listed in Table 1.

The reproducibility was ascertained by measuring the experimental data on several samples prepared under nearly identical conditions. All the films prepared have a thickness of 0.35–0.4 μm as estimated by the Stylus profilometer (Mitutoyo). The structural aspects were investigated by X-ray diffraction (XRD) (PANalytical-3040 X'pert Pro) using CuKα radiation ($\lambda = 1.5414$ Å). To obtain information on the surface chemistry of the prepared films, Fourier transform infrared (FT-IR) transmittance spectrum was recorded between 400 and 4000 cm^{-1} using Thermo Nicolet Nexus spectrometer. Optical transmittance measurements were performed with a Hitachi-330 UV–vis-NIR spectrophotometer in the range of $\lambda = 280$–1500 nm. The sheet resistance and conductivity were measured using the conventional four-probe method at different temperatures (30–100 °C). The effective carrier concentration and mobility were calculated using Hall effect measurements. Microstructural features and surface morphology of the deposited films were investigated using Philips scanning electron microscope (SEM) and atomic force microscope (AFM).

Table 1
Optimized spray deposition conditions for preparing spinel $MgIn_2O_4$ films

Spray parameters	Values/quantity
Solvent ethanol (%)	100
Substrate temperature (°C)	400–450
Carrier gas flow rate ($kg\,cm^{-2}$)	0.4
Substrate to nozzle distance (cm)	30
Time of deposition (min)	10
Precursor flow rate ($ml\,min^{-1}$)	2.5

3. Results and discussion

The XRD pattern of the film prepared at 400 and 450 °C for the stoichiometric ratio 1:2 (Mg:In) is shown in Fig. 1a and b, respectively. The XRD pattern of the powdered $MgIn_2O_4$ sample is also shown for comparison (Fig. 1c). The observed interplanar distances between the planes of the crystal lattice were compared with the standard data (JCPDS 73-2414) and are listed in Table 2 for comparison. Each peak in the diffraction pattern of the spray deposited film was completely indexed by assuming single-phase $MgIn_2O_4$ spinel structure. The XRD indicates clearly that the high temperature growths do have better crystallinity. Also noted that no characteristic peaks of impurity and dopant phases have been observed. Further, it shows the polycrystalline nature of the film with (3 1 1) preferred orientation. The lattice constant was calculated from the intense peak emerged from the lattice plane indexed (3 1 1). The unit cell dimension of the grown thin films at 450 °C was found to be 8.884 Å, which is comparable to the standard value 8.864 Å. The full-width at half-maximum of the (3 1 1) diffraction peak was used to estimate the crystallite dimension using Scherrer's equation, which was found to be 52 nm for the films deposited at 450 °C. Details about dislocation density, lattice strain and number of crystallites calculated for all orientations are also listed in Table 2.

The interaction between the different components of the films was further investigated by FT-IR spectroscopy. Fig. 2 shows the FT-IR transmission spectrum of the $MgIn_2O_4$ films deposited on glass substrate at 450 °C. The weak peak at 1275 cm^{-1} was assigned to the vibration absorption of the In–OH bond in $In(OH)_3$ [20]. These bands are due to hydration usually originated from the precursor and solvent or from exposure to the atmosphere. Two absorption peaks appeared at the finger print region 561 and 404 cm^{-1}, which are associated with the longitudinal optical phonon modes for the metal-oxide stretching. This implies that the films consist mostly of $MgIn_2O_4$.

The values of electrical conductivity (σ), carrier density (n) and mobility (μ) were obtained from the combined measurement of resistivity and Hall coefficient. The dc

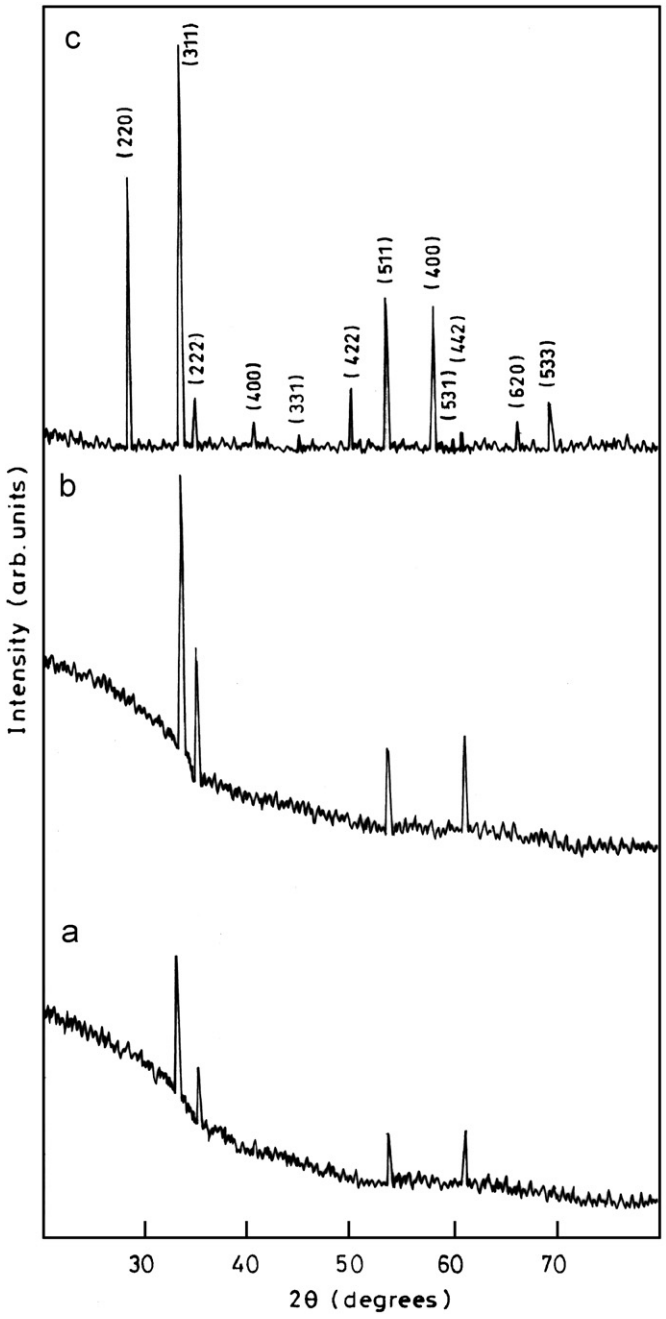

Fig. 1. XRD pattern of spray pyrolytically prepared $MgIn_2O_4$ thin films at (a) 400 °C, (b) 450 °C and (c) for the $MgIn_2O_4$ powder sample.

electrical conductivity of the prepared MIO films was measured in the temperature range between 30 and 150 °C by the four-probe technique. Silver electrodes were provided on the sample and were contacted by Cu wires. The conductivities of the prepared samples as a function of temperature are shown in Fig. 3.

It is noted that conductivity of the film deposited at 450 °C is in the order of $0.15–1.24 \times 10^{-4}\,S\,cm^{-1}$ in the measured temperature range. Their temperature dependence of conductivity shows the degenerate semiconductor behavior with less electrical conductivity variations [13]. Its conductivity is attributed to carrier generation that strongly depends on the preparation parameters which make the film more crystalline. In addition, as the concentration of the conduction electrons became higher, Fermi energy level seems to be shifted upward that gears the conduction behavior. However, the samples prepared at 400 °C showed stronger temperature dependence than that of the samples deposited at 450 °C and have less electrical conductivity in the range of $0.56–3.24 \times 10^{-5}\,S\,cm^{-1}$. This result shows that the resistivity of the MIO films decreases with the increase of substrate temperature. Further, it signifies that both dislocation and grain boundary densities decrease as the deposition temperature increases, there by reducing the number of scattering centers which enhances carrier concentration leading to high conductivity. The measured conductivity may be fitted with the following expression:

$$\sigma = \sigma_0 \exp\left(\frac{-E_a}{kT}\right), \tag{1}$$

where σ_0 is a constant, k is Boltzmann constant, T is temperature in K and E_a is the activation energy. From the slope of the curve, the activation energy values are found to be 0.765 and 0.57 eV for the MIO films prepared at 400 and 450 °C, respectively. The lower activation energy value associated with the $MgIn_2O_4$ films formed at 450 °C confirms the formation of well-crystallized lattices with high conductivity [20].

Measurement of Hall effect showed that the carrier is an electron (n-type) which are generated from interstitial or substituted cations and/or oxygen vacancies. The carrier concentration is measured and found to be in the order of $2.7 \times 10^{19}\,cm^{-3}$ for the MIO films prepared at 450 °C which is slightly higher than $1.9 \times 10^{19}\,cm^{-3}$ for the films prepared at 400 °C.

Even though the carrier concentration is high, the as-deposited $MgIn_2O_4$ film deposited at 450 °C has low electrical conductivity of about $10^{-4}\,S\,cm^{-1}$ at RT. The overall lower conductivity should be attributed to the stoichiometric nature of these films that show better crystallinity with low values of carrier mobility in the range of $10^{-3}\,cm^2\,V^{-1}\,s^{-1}$. However, the observed mobility value of $9.5 \times 10^{-3}\,cm^2\,V^{-1}\,s^{-1}$ for the film deposited at 450 °C is higher than that of $0.3 \times 10^{-3}\,cm^2\,V^{-1}\,s^{-1}$ for the films deposited at 400 °C. This temperature-dependent behavior of mobility is the primary cause for the observed increase of conductivity with spray temperature. This is similar to the reported electrical behavior of $MgIn_2O_4$ spinel pellet sintered at 1500 °C [21].

These electrical properties elucidate that the carrier concentration mainly depends on the available oxygen vacancies in the spray prepared films. From Fig. 3 it is also found that conductivity of the MIO film increases with temperature and these variations may be mainly due to the change in the concentration of the conduction electrons, which might have probably produced by oxygen vacancies. The electrical conductivity of oxide semiconductors is mainly determined from the charge carrier concentration of

Table 2
Structural parameter of $MgIn_2O_4$ thin film deposited at 400 and 450 °C

Specimen details	Diffraction angle (2θ) deg	(h k l)	Observed d_{hkl} (Å)	Standard d_{hkl} (Å)	Grain size (nm)	Dislocation density ($\times 10^{14}$ lines m^{-2})	No. of crystallites ($\times 10^{15}$ m^3)	Micro strain ($\times 10^{-4}$)
$MgIn_2O_4$ deposited at 400 °C	33.3196	(3 1 1)	2.687	2.673	49	4.16	3.39	6.57
	34.8043	(2 2 2)	2.576	2.558	37	7.24	7.79	8.32
	53.4104	(5 1 1)	1.7140	1.809	22	21.08	38.72	9.44
	62.5814	(4 4 2)	1.483	1.498	23	19.47	34.37	7.82
$MgIn_2O_4$ deposited at 450 °C	33.4261	(3 1 1)	2.679	2.673	52	3.73	2.88	6.2
	34.9105	(2 2 2)	2.568	2.558	43	5.32	4.91	7.11
	53.5163	(5 1 1)	1.706	1.809	23	18.64	3.22	8.87
	62.6910	(4 4 2)	1.481	1.498	24	17.61	2.96	7.46

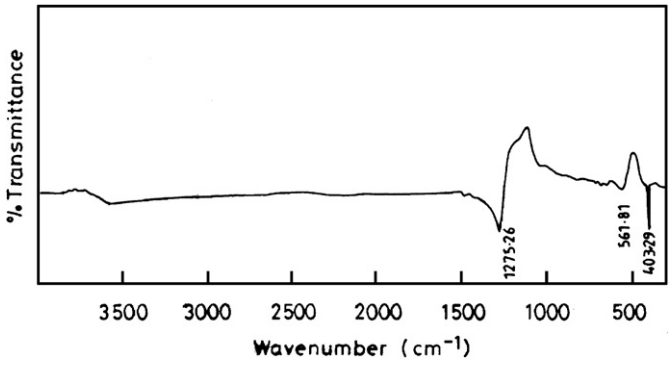

Fig. 2. FT-IR spectrum of the sprayed $MgIn_2O_4$ sample at 450 °C.

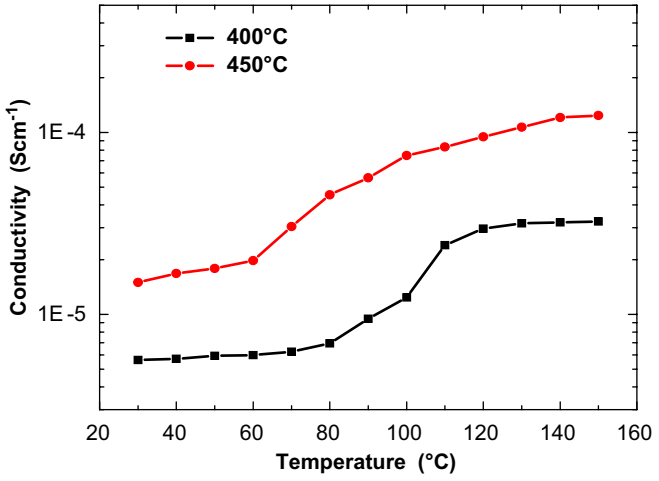

Fig. 3. Electrical conductivity variation of MIO films with temperature.

electrons (n) and their mobility (μ), both being governed by the cation stoichiometry and oxygen vacancy. As far as the $MgIn_2O_4$ spinel films prepared by the spray pyrolysis technique here, the X-ray results show the formation of stoichiometric and well-crystallized films without the presence of either metallic Mg, In, or MgO or In_2O_3 oxide phases. Here, the observed moderate conductivity values of 10^{-4}–10^{-5} S cm^{-1} may be attributed only to the oxygen vacancies produced at higher temperatures. The oxygen vacancies act as doubly ionized donors and each vacancy contributes two electrons to the electrical conduction as evident from the reaction:

$$O_0 \rightarrow V_0^- + 2e^- + \tfrac{1}{2}O_2(g). \quad (2)$$

The optical properties of magnesium indate films are characterized from the transmittance spectra (Fig. 4). The films deposited at 450 °C has an average optical transmission of ~75% in the visible wavelength range 500 nm, without any absorption in the visible and IR region. The optical bandgap of $MgIn_2O_4$ were also estimated from the transmittance data.

The absorption co-efficient 'α' is calculated from the transmittance spectrum using the relation

$$\alpha = -\frac{\log_e(1/T)}{t}, \quad (3)$$

where T is the optical transmittance. The absorption coefficient of the film was found to be of the order of 10^4 cm^{-1} which exponentially decreases as phonon energy decreases.

In order to confirm the nature of optical transition in the prepared films, the optical data were analyzed using the equation

$$\alpha = \frac{\alpha_0(h\nu - E_g)^n}{h\nu}, \quad (4)$$

where E_g is the separation between bottom of conduction band and top of the valence band, $h\nu$ is the photon energy and n is the constant, which varies with the nature of transition.

For allowed direct transition $n = \frac{1}{2}$ and for allowed indirect transition $n = 2$. The plot of $(\alpha h\nu)^2$ against $h\nu$ for the MIO film deposited at 450 °C is shown in Fig. 4b. The nature of the plots suggests direct interband transition. The straight line in this figure was extrapolated to $\alpha = 0$ and the energy-axis intercept were considered to be the E_g value. The optical bandgap of $MgIn_2O_4$ is found to be 3.82 eV, which is greater than that of $MgIn_2O_4$ powder (3.45 eV) synthesized by the ceramic route [7]. The increased

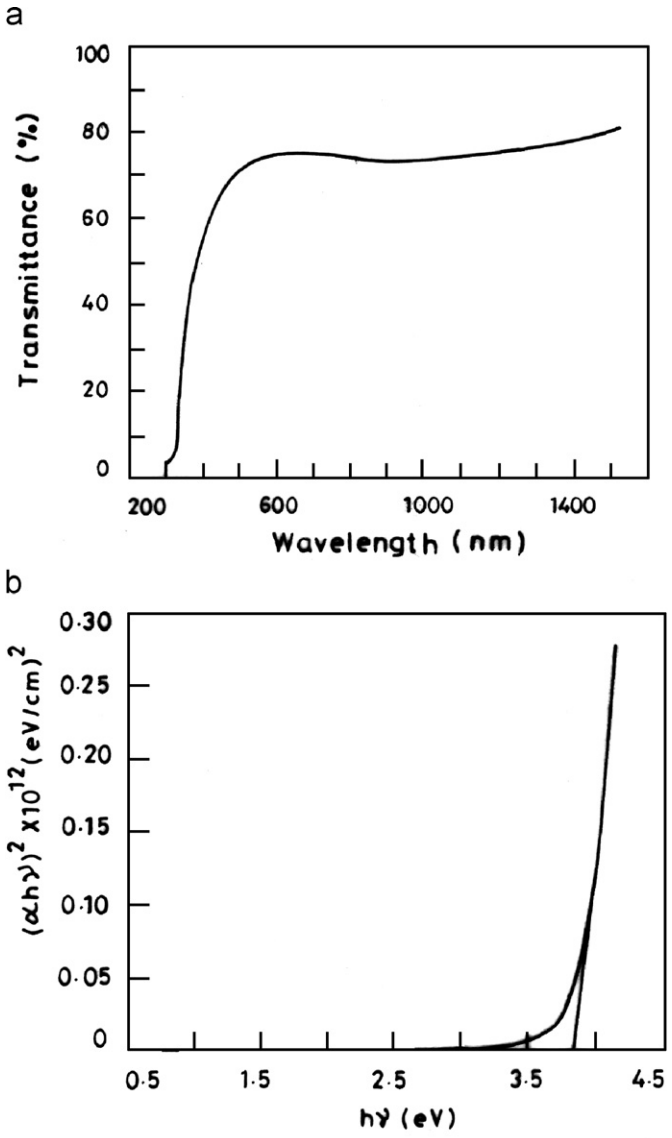

Fig. 4. (a) Optical transmittance of the $MgIn_2O_4$ film deposited at 450 °C and (b) $h\nu$ vs. $(\alpha h\nu)^2$ curve extrapolated to observe the optical bandgap.

bandgap value may be attributed to the larger crystallite size and this higher energy gap value makes the sprayed $MgIn_2O_4$ film a novel transparent and conducting oxide material for optoelectronic devices.

Similar studies have been performed for the films deposited at 400 °C and the transmittance was found to be 67% and the optical bandgap value is about 3.75 eV. Observed electrical and optical constants are tabulated in Table 3.

Fig. 5 shows the SEM images of the $MgIn_2O_4$ films deposited on glass substrates at 400 and 450 °C. The film is dense, uniform and crack-free indicating that film deposition using spray pyrolysis is effective in achieving crack-free magnesium indate films. In sol–gel growth, usually cracks are very easily developed from strain due to the fragile nature of the sol. Furthermore, more cracks can develop due to large volume shrinkage. In the case of spray deposition, however, the sprayed liquid clusters are gelled, calcined and crystallized during deposition, which can release the strain sufficiently during processing. The smoothness of the spinel layer is proved by the obtained SEM images with a magnification of 20 K. The particles in

Table 3
Electrical and optical datas of the $MgIn_2O_4$ films deposited at different substrate temperature

Parameters	$MgIn_2O_4$ films deposited at 400 °C	$MgIn_2O_4$ films deposited at 450 °C
Conductivity ($S\,cm^{-1}$)	$0.56–3.24 \times 10^{-5}$	$0.15–1.24 \times 10^{-4}$
Activation energy (eV)	0.765	0.57
Carrier concentration (cm^{-3})	1.9×10^{19}	2.658×10^{19}
Mobility ($cm^2\,V^{-1}\,s^{-1}$)	0.29×10^{-3}	9.5×10^{-3}
Transmittance (%)	67	75
Optical band gap (eV)	3.75	3.82

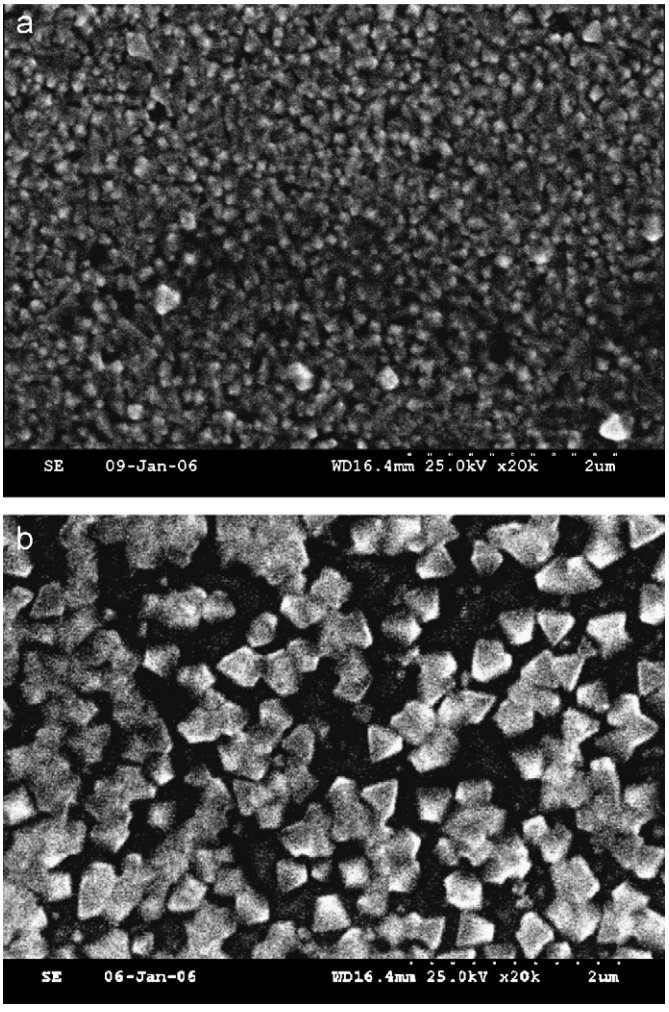

Fig. 5. SEM micrograph of the sprayed $MgIn_2O_4$ films deposited at (a) 400 °C and (b) 450 °C.

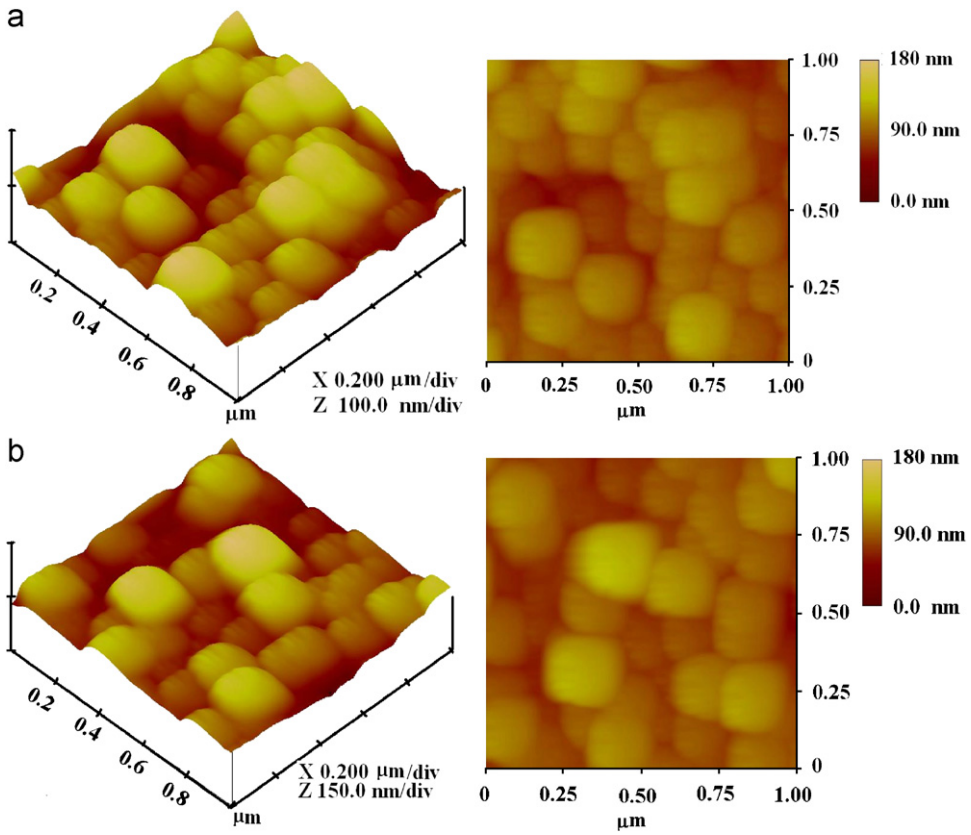

Fig. 6. AFM micrographs of the $MgIn_2O_4$ films deposited at (a) 400 °C and (b) 450 °C.

the film are uniform crystallites of pyramidal type, about 250 nm in size. These pyramidals are distributed uniformly throughout the film with the above size, which is larger than indicated by the XRD pattern. It was noted that the grain size of the films deposited at 450 °C are higher than that of the films prepared at 400 °C leading to better surface smoothness.

AFM was used to observe the surface morphological characteristics of the films. Recorded images have been used for image analysis and quantitative interpretation of the surface characteristics (surface roughness and grain size evaluation). Fig. 6 shows the 2D and 3D AFM images of MIO spinel films deposited at different substrate temperatures 400 and 450 °C. A quantitative analysis of the surface roughness upon the images, by using the root-mean-square (RMS) function of the nanoscope III, DI software [22] was performed. RMS is defined as the standard deviation of the surface heights calculated from all points obtained during a given scan [23]. These values were used to indicate the film surface roughness quantitatively. The obtained RMS results, by averaging the images over an area of 1 µm, are given in Table 4. The RMS of the 450 °C deposited films markedly decreased up to 5.6 nm and the lateral size of the round-shape domain was also enlarged, compared with the other $MgIn_2O_4$ films deposited at 400 °C.

Additional information has been obtained that all columns are of the same shape and size. They are of spherical shape with sides in the range of 150–250 nm. On

Table 4
Results of the surface roughness and the grain size analysis of the $MgIn_2O_4$ films deposited at different substrate temperature

Sample details	RMS roughness (nm)	Grain size (nm)
MIO films deposited at 400 °C	18.5	184
MIO films deposited at 450 °C	5.6	234

average, the grain size are 184 and 234 nm for the $MgIn_2O_4$ films deposited at 400 and 450 °C, respectively, which indicates that the surfaces of the film grown are smooth, homogeneous and parallel to the substrate flat surface. The grain size value was comparable to that obtained through the SEM studies. The grain size of the film deposited at 400 °C is smaller than those of the films deposited at 450 °C. This result is confirmed in the optical studies that films with larger grain size exhibit higher transmittance.

4. Conclusion

Well-crystallized $MgIn_2O_4$ thin films were prepared using spray pyrolysis deposition technique on glass substrates for the first time. Stoichiometrically prepared films at 450 °C were polycrystalline with intense peak along (3 1 1) orientation with thickness between 0.36 and 0.40 µm.

Dc electrical conductivity and carrier concentration of the films increased slightly with substrate temperature. The maximum electrical conductivity of $1.24 \times 10^{-4}\,S\,cm^{-1}$ was achieved for the films deposited at 450 °C. High concentration of electron carriers ($2.70 \times 10^{19}\,cm^{-3}$) was introduced into the film from the oxygen vacancies. Even though the carrier concentration is high enough for electrical conduction, the resulted films have low electrical conduction in the order of 10^{-4}–$10^{-5}\,S\,cm^{-1}$. This may be due to the lower mobility of the carriers due to scattering within the grain boundaries. The optical bandgap of the deposited films at 450 °C is 3.82 eV which is greater than the doped indium oxide (ITO) films. Increasing the substrate temperature from 400 to 450 °C improves the crystallinity and the optical transmittance whereas decreases the electrical resistivity. From the electrical, optical characterization and their surface morphology through SEM and AFM micrographs, it is obvious that the MIO films deposited by spray pyrolysis at these optimized conditions are suitable for electronic applications, especially for those devices requiring transparent as well as conducting electrodes.

References

[1] I. Hamberg, C.G. Granqvist, J. Appl. Phys. 60 (1986) R123.
[2] T. Minami, H. Sato, H. Nanto, S. Takata, Jpn. J. Appl. Phys. 24 (1985) L781.
[3] Y. Dou, G. Egdell, Phys. Rev. B 53 (1996) 15405.
[4] K. Budzynska, E. Leja, S. Skrztpek, Sol. Energy Mater. 12 (1985) 57.
[5] D.R. Kammler, T.O. Mason, D.L. Young, T.J. Coutts, D. Ko, K.R. Poeppelmerer, D.L. Williamson, J. Appl. Phys. 90 (2001) 5979.
[6] H. Kawazoe, N. Ueda, H. Un'no, T. Omata, H. Hosono, H. Tanoue, J. Appl. Phys. 76 (1994) 7935.
[7] N. Ueda, T. Omata, N. Hikuma, K. Udea, H. Mizoguchi, T. Hashimoto, H. Kawazoe, Appl. Phys. Lett. 61 (1992) 1954.
[8] T. Omata, N. Ueda, N. Hikuma, K. Udea, H. Mizoguchi, T. Hashimoto, H. Kawazoe, Appl. Phys. Lett. 62 (1993) 499.
[9] T. Omata, N. Ueda, K. Ueda, H. Hawazoe, Appl. Phys. Lett. 64 (1994) 1077.
[10] H. Enoki, T. Nakayama, J. Echigoya, Phys. Status Solidi (a) 129 (1992) 181.
[11] P.M. Sirimanne, N. Sonoyama, T. Sakata, J. Solid. State Chem. 154 (2000) 476.
[12] S.-H. Wei, S.B. Zhang, Phys. Rev. B 63 (2001) 45112.
[13] H. Un'no, N. Hikuma, T. Omata, N. Ueda, T. Hashimoto, Kawazoe, Jpn. J. Appl. Phys. 32 (1993) 1260.
[14] A. Kudo, H. Yanagi, H. Hosono, H. Kawazoe, Mater. Sci. Eng. B 54 (1998) 51.
[15] N. Ueda, T. Omata, N. Hikuma, K. Ueda, H. Mizoguchi, T. Hashimoto, H. Kawazoe, Appl. Phys. Lett. 61 (1992) 1954.
[16] T. Minami, S. Takata, T. Kakumu, H. Sonohara, Thin Solid Films 270 (1995) 22.
[17] H. Un'no, N. Hikuma, T. Omata, N. Ueda, T. Hashimoto, H. Kawazoe, Jpn. J. Appl. Phys. 32 (1993) L1260.
[18] H. Hosono, H. Un'no, N. Ueda, H. Kawazoe, N. Matsunami, H. Tanoue, Nucl. Instr. and Meth. Phys. Res. B 106 (1995) 517.
[19] J.J. Prince, S. Ramamurthy, B. Subramanian, C. Sanjeeviraja, M. Jayachandran, J. Crystal Growth 240 (2002) 142.
[20] A.R. West, Solid State Chemistry and its Applications, Wiley, Singapore, 2004.
[21] H. Tanji, N. Kurihara, M. Yoshide, J. Mater. Sci. Lett. 13 (1994) 1673.
[22] Digital Instruments, Nanoscope III, Owner's Manual.
[23] Y.G. Li, A. Lusia, J. Appl. Electrochem. 27 (1997) 643.